BBA - Biomembranes 1867 (2025) 184396

Contents lists available at ScienceDirect

BBA - Biomembranes

journal homepage: www.elsevier.com/locate/bbamem

Voltage- and Ca^{2+}-inducible PLC activity for analyzing $PI(4,5)P_2$ sensitivity of ion channels in *Xenopus* oocytes

Takafumi Kawai [a,*], Natsuki Mizutani [a,b], Yasushi Okamura [a,c]

[a] Graduate School of Medicine, Osaka University, Japan
[b] Institute for Protein Research, Osaka University, Japan
[c] Graduate School of Frontier Biosciences, Osaka University, Japan

ARTICLE INFO

Keywords:
PLCζ
Ion channel
Membrane potential
Calcium
Xenopus oocyte

ABSTRACT

Phosphatidylinositol 4,5-bisphosphate (PIP_2) is a key membrane lipid regulating various ion channel activities. Currently, several molecular tools are used to modulate PIP_2 levels, each of which has distinct advantages and drawbacks. In this study, we proposed a novel methodology using heterologous *Xenopus* oocytes to precisely manipulate PIP_2 levels using phospholipase C (PLC)-ζ, which hydrolyzes PIP_2. *Xenopus* oocytes injected with PLCζ exhibited notable hyperpolarization-induced Ca^{2+} influx driven by the increased driving force of Ca^{2+}. High Ca^{2+} sensitivity of PLCζ facilitated hyperpolarization-induced PLC activity in *Xenopus* oocytes that was voltage- and Ca^{2+}-dependent. This study demonstrated the regulatory capacity of PLCζ in modulating PIP_2-sensitive ion channels, such as the KCNQ2/3 and GIRK channels, in a voltage- and Ca^{2+}-dependent manner. Moreover, activation pathway of PLCζ only requires a two-electrode voltage clamp setup, making it a convenient molecular tool to manipulate PIP_2 levels in combination with a voltage-sensing phosphatase (VSP). PLCζ has distinct characteristics and advantages compared to VSP: (1) Hyperpolarization, but not depolarization, reduced the PIP_2 levels, (2) PIP_2 levels were decreased without any increase in phosphatidylinositol 4-monophosphate (PIP) levels, and (3) PIP_2 levels were reduced by Ca^{2+} administration. Therefore, PLCζ effectively supports understanding how PIP_2 regulates ion channels, alongside VSP. Overall, this study highlights the unique characteristics of PLCζ and its distinct advantages in analyzing ion channel regulation by PIP_2 and the PLC pathway in *Xenopus* oocytes.

1. Introduction

Plasma membrane plays a crucial role in various physiological processes and its lipid composition is a critical determinant of its functionality. Among the diverse lipid species constituting the cell membrane, phosphatidylinositol 4,5-bisphosphate (PIP_2) is a key regulator of several physiological phenomena, including cell signaling, cytoskeletal dynamics, and membrane trafficking [1,2]. Dynamic changes in PIP_2 levels also play important roles in regulating the functions of ion channels [3,4], as exemplified by the M-current, which is mediated by the activation of muscarinic acetylcholine receptors and closure of PIP_2-sensitive KCNQ2/3 channels [5,6]. Currently, over 50 ion channels have been reported to exhibit PIP_2 sensitivity, underscoring the diverse roles of PIP_2 in ion channel regulation [3,7–9].

Various strategies have been developed to manipulate the PIP_2 content in the plasma membrane and explore the diverse mechanisms of ion channel regulation by PIP_2 [8,10,11]. For instance, voltage-sensing phosphatase (VSP) is extensively used to investigate PIP_2-dependent ion channel gating; it facilitates rapid PIP_2 conversion into phosphatidylinositol 4-phosphate (PIP) in a voltage-dependent manner [8,12]. Alternatively, based on the same principle as the M-current described above, the classical approach expresses the muscarinic acetylcholine receptor and applies agonistic stimulation [6], activating the PLC pathway to cleave PIP_2. Furthermore, chemogenetic tools, such as rapamycin-mediated pseudojanin (PJ) [13,14], and optogenetic tools using the CRY2/CIBN system [15] have also been developed to manipulate plasma membrane PIP_2 levels. Currently, many of these tools are used for ion channel analysis.

However, considering the diverse principles of these tools and their individual characteristics (e.g., PIP_2 hydrolysis, dephosphorylation, voltage-dependence, chemogenetics, and optogenetics), each tool has unique advantages and disadvantages in investigating ion channel

* Corresponding author at: Laboratory of Integrative Physiology, Graduate School of Medicine, Osaka University, Suita, Osaka 565-0871, Japan.
E-mail address: kawai@phys2.med.osaka-u.ac.jp (T. Kawai).

https://doi.org/10.1016/j.bbamem.2024.184396
Received 18 July 2024; Received in revised form 19 October 2024; Accepted 23 October 2024
Available online 30 October 2024

function (Table 1). Owing to the inherent diversity in the properties of ion channels, such as voltage dependency, gating mechanism, and kinetics, appropriate tools should be selected based on the physiological nature of individual ion channels.

Expanding the repertoire of tools for PIP_2 concentration regulation has recently gained attention. In this study, we established a novel approach for PIP_2 manipulation using heterologous *Xenopus* oocytes, a widely used system to study the physiological properties of ion channels. Our methodology focuses on PLCζ, which hydrolyzes PIP_2 in a calcium-dependent manner [16,17]. Interestingly, introduction of PLCζ into *Xenopus* oocytes alone induced Ca^{2+} increase in response to hyperpolarization, which increases the driving force of Ca^{2+}, consistent with observations in oocytes injected with IP_3, a downstream effector of PLC [18]. Store-operated calcium entry (SOC) facilitates Ca^{2+} influx upon hyperpolarization due to the enhanced driving force, whereas depolarization induces the opposite effect. As PLCζ activity is regulated by Ca^{2+}, PLCζ expression induces voltage- and calcium-dependent PLCζ activity in *Xenopus* oocytes.

In this study, we compared the advantages and disadvantages of our novel technique with other PIP_2-manipulating tools, emphasizing its potential contribution to the expanding field of ion channel regulation.

2. Methods

2.1. Plasmid and RNA synthesis

Open reading frame of PLCζ was subcloned from mouse testis cDNA into the pSD64TF vector. Errors that differed from those in the database (NM_054066.4) were corrected via single-nucleotide mutagenesis (PrimeSTAR Max; Takara, Shiga, Japan). We also constructed a mutant that canceled the charge of the basic amino acid cluster [19] by changing 374–379 of KKRKRK to NNQNQN. Polymerase chain reaction (PCR) was performed using PrimeSTAR Max with the following primers using PLCζ in pSD64TF as a template. Fw, AACAATCAAAACCAGAACATGAAAATAGCCATGGCCTTA; Rv, GTTCTGGTTTTGATTGTTGACGCCTGCTATTCCACTCAATG.

After DpnI treatment (Takara), transformation was performed to obtain the desired mutant. In the western blotting experiment, hemagglutinin (HA)-tagged sequence was incorporated at the C-terminus of PLCζ. KCNQ2/3 plasmids were generously provided by Dr. David McKinnon (Stony Book University, NY, USA) and Dr. Koichi Nakajo (Jichi Medical University, Shimotsuke, Japan). GIRK2d plasmid was contributed by Dr. Yoshihisa Kurachi (Osaka University, Suita, Japan), and G-protein β1 and γ1 subunit plasmids were provided by Dr. Toshihide Nukada (retired). The plasmid of the GFP-fused pleckstrin homology domain from the PLCδ subunit (PHPLCδ-GFP) was the same as that used in previous study [20]. G-CaMP 8 plasmid was provided by Dr. Masamichi Ohkura (Saitama University, Saitama, Japan) and transferred to pSD64TF for complementary RNA (cRNA) synthesis. cRNA was synthesized using the mMESSAGE mMACHINE transcription kit (Thermo Fisher Scientific, MA, USA) following linearization with restriction enzymes.

2.2. Xenopus oocyte preparation and electrophysiological recording

Xenopus oocytes were obtained from anesthetized animals submerged in ice-cold water containing 0.2 % ethyl 3-aminobenzoate methanesulfonate salt (Tokyo Chemical Industry, Tokyo, Japan). Follicular cells were removed via defolliculation, by treating with collagenase P (1.0 mg/mL; Roche, Basel, Switzerland) in an ND96 solution containing 96 mM NaCl, 2 mM KCl, 5 mM HEPES, 1.8 mM $CaCl_2$, and 1 mM $MgCl_2$ (pH 7.5). Subsequently, defolliculated oocytes were injected with cRNA. The synthesized cRNA was diluted as follows: PLCζ (150 ng/μL), KCNQ2/3 (30 ng/μL for each), and GIRK2d (100 ng/μL) with bovine G-protein β1 and γ1 (100 ng/μL). Approximately 50 nL of cRNA was injected into the defolliculated oocytes. Then, oocytes were incubated with ND96 solution supplemented with 0.1 mg/mL gentamycin (Nacalai Tesque, Japan) and 5 mM sodium pyruvate for two days. However, in PLCζ co-expression experiments with KCNQ2/3 and GIRK, the cells were incubated with low Ca^{2+} solution containing 83.7 mM NaCl, 2 mM KCl, 0.16 mM $CaCl_2$, 1 mM $MgCl_2$ and 5 mM HEPES (pH 7.5) to reduce toxicity. Two days post-cRNA injection, currents were recorded using the two-electrode voltage clamp (TEVC) technique and OC-725 amplifier (Warner Instruments, Hamden, CT, USA). The

Table 1
A list of methodologies for regulating PIP_2.

Name	Methodology	Equipment	Advantage	Disadvantage	Reference
Inside-out patch	1. Perform inside-out patch clamp recording 2. Apply soluble short acyl chain PIP_2 to the inner leaflet	1. Patch clamp 2. Rapid perfusion system	1. Highly quantitative 2. Can identify the selectivity of phosphoinositides (PIPs) 3. Applicable to rapidly inactivating ion channels	1. Potential difference between soluble and native PIP_2 2. Requires the rapid perfusion system	[29]
VSP	1. Co-express VSP with the target channels 2. Apply depolarizing pulse to activate VSP; PIP_2 is converted to PIP	1. Patch clamp or TEVC	1. Simple equipment 2. Quick response to depolarization 3. Reversible response	1. Difficult to use for rapidly inactivating ion channels 2. Instead of PIP_2 reduction, PIP is upregulated	[12]
G_qPCR	1. Co-express G_qPCR with the target channels 2. Apply the ligand to activate the G_qPCR pathway	1. Patch clamp 2. Perfusion system	1. PIP_2 is cleaved with no PIP production 2. Applicable to rapidly inactivating ion channels	1. Gq pathway is activated (Ca^{2+} levels increase) 2. Requires ligands for activation 3. Reports on *Xenopus* oocytes are limited	[6]
Pseudojanin (PJ)	1. Co-express PJ and Lyn11-FRB with the target channels 2. Apply rapamycin to translocate PJ to the plasma membrane	1. Patch clamp or TEVC 2. Perfusion system	1. Both PIP_2 and PIP can be reduced 2. Applicable to rapidly inactivating ion channels	1. No recovery after rapamycin treatment 2. Requires ligands for activation	[13]
CRY2/CIBN System	1. Co-express CIBN-CAAX and CRY2–5-$ptase_{OCRL}$ with the target channels 2. Apply blue light illumination; PIP_2 is converted to PIP	1. Patch clamp or TEVC 2. Optogenetics system	1. Applicable to rapidly inactivating ion channels 2. Reversible response	1. Requires optogenetics system	[15]
PLCζ	1. Co-express PLCζ with the target channels 2. Apply hyperpolarization pulse to activate PLCζ	1. TEVC 2. Perfusion system (optional)	1. Simple equipment 2. Either voltage or calcium can be used for PLCζ activation 3. PIP_2 is cleaved without PIP production	1. Not applicable to Ca^{2+}-sensitive channels 2. PLC pathway is activated	

recordings were performed in ND96, unless otherwise noted. Low-Cl ND96 solution contained 96 mM Na-gluconate, 2 mM KCl, 5 mM HEPES, 1.8 mM $CaCl_2$, and 1 mM $MgCl_2$ (pH 7.5). $CaCl_2$ was added to obtain the indicated concentration. ND100 solution contained 100 mM NaCl, 2 mM KCl, 5 mM $MgCl_2$, and 5 mM HEPES (pH 7.6), and $CaCl_2$ was added to reach the indicated concentration. Data acquisition was accomplished with an AD/DA converter, Digidata 1440A (Molecular Devices, San Jose, CA, USA) or InstruTECH LIH 8 + 8 (HEKA Elektronik, Lambrecht, Germany), operating under pClamp (Molecular Devices) or PatchMaster software (HEKA Elektronik) at a room temperature of 22–24 °C. The output signals were digitized at a rate of 10 kHz. Glass electrodes, which were filled with 3 M KCl or 10 mM KCl + 3 M K-acetate, with resistance ranging from 0.2 to 1.0 MΩ, were used for the experiments.

2.3. Voltage clamp fluorometry (VCF) recording with PHPLCδ-GFP or G-CaMP 8

cRNA encoding the green fluorescent protein (GFP)-fused pleckstrin homology domain from the PLCδ subunit (PHPLCδ-GFP) or G-CaMP 8 was used for subsequent tests. In PHPLCδ-GFP experiments, oocytes were incubated with ND100 + 0.2 mM Ca^{2+} for two days post-cRNA injection. Live cell imaging was performed using the Olympus BX50WI upright fluorescence microscope equipped with a water-immersed 20 × 1.00 N.A. objective lens and LED lamp (MCWHL8; Thorlabs, Inc., USA). The illumination system included an excitation filter BP460-480HQ (Olympus) and emission filter BA495-540HQ (Olympus). The emitted light from the entire surface within the field of view was detected using a photomultiplier tube (PMT; H10722-20; Hamamatsu Photonics, Hamamatsu, Japan). The output signals from PMT were digitized at 10 kHz with the AD/DA converter (Digidata 1440A) and analyzed using the pClamp software. Voltage clamp was performed using an Oocyte Clamp amplifier (OC-725C) with Digidata 1440A and pClamp software. ND96 was used as the bath solution, unless otherwise noted. For the calculation of fluorescence changes due to membrane potential changes (Fig. 2, Fig. S2 and Fig. S3), the average value was calculated over a 0.1-s range just before the pulse was applied or just before the pulse ended. The glass electrodes were filled with 3 M K^+-acetate and 10 mM KCl with resistance of 0.2–1.0 MΩ. The signals were low-pass filtered at 100 Hz.

2.4. Western blotting

Xenopus oocytes injected with PLCζ-HA cRNA were incubated for two days in ND96. Ten cells were washed twice with PBS and sonicated in 50 mL of PBS containing complete protease inhibitor cocktail tablets without EDTA (Roche, Basel, Switzerland) for 30 s. After centrifugation (500 ×*g* for 5 min at 4 °C), the supernatant was obtained as a lysate. The lysate was incubated with the sodium dodecyl sulfate-polyacrylamide gel electrophoresis buffer containing 5 % 2-ME and boiled for 5 min at 96 °C.

Then, the proteins were transferred onto polyvinylidene fluoride membranes. After blocking with 0.5 % skim milk, the blots were incubated with anti-HA (1:2000; Covance, Berkeley, CA, USA) in Can Obtain Signal 1 Immunoreaction Enhancer Solution (Toyobo, Osaka, Japan), washed, and incubated again with horseradish peroxidase-conjugated anti-mouse antibody (1:2000; Cytiva, Marlborough, MA, USA) in Can Get Signal 2 Immunoreaction Enhancer Solution (Toyobo). Signals were detected using the ECL Prime Western Blotting Detection Reagent (Cytiva). Images were acquired using the CS analyzer system version 3 (ATTO, Tokyo, Japan).

2.5. Data analyses

Data analyses were conducted using Excel 2016 (Microsoft, Redmond, WA, USA), Clampfit 10.5 (Molecular Devices), and Igor Pro 6.37 (WaveMetrics, Portland, OR, USA). Statistical analyses were conducted using Prism 6 (GraphPad Software, San Diego, CA, USA). For two-group comparisons, an unpaired *t*-test was used. Data are represented as the mean ± standard error of the mean. Statistical significance was set at $*p < 0.05$, $**p < 0.01$, and $****p < 0.0001$.

3. Results

3.1. Intracellular calcium levels change in a voltage-dependent manner in PLCζ-injected Xenopus oocytes

After we confirmed that HA-tagged PLCζ is successfully expressed in *Xenopus* oocytes using western blotting (Fig. 1A), we expressed PLCζ and conducted two-electrode voltage clamp (TEVC) recording in ND96 solution (Fig. 1B). We unexpectedly observed that PLCζ-injected oocytes exhibited a huge outward current at +50 mV stepped from −100 mV, which was never observed in uninjected control (Fig. 1C–D). We also confirmed that this current is not observed in PLCζ mutant that lacks the positive charge potentially necessary for the membrane binding [19] (Fig. 1C–D) in spite of its protein expression in oocytes (Fig. S1). Because the trace appearance in PLCζ WT-injected oocytes was similar to the already known calcium-activated Cl^- channels (CaCCs), which are sometimes observed in *Xenopus* oocytes [21], we changed the extracellular Cl^- from 103.6 mM to 5 mM (Fig. 1E). As a result, the outward current amplitude was drastically reduced, and the reversal potential of the tail current was positively shifted from −11.3 mV to +57.4 mV by this manipulation (Fig. 1E). Furthermore, this current was suppressed by Ani9 treatment (Sigma, St. Louis, MO, USA), which inhibits TMEM16A (Fig. 1F), a type of CaCC expressed in *Xenopus* oocytes [22]. These results indicated that the current observed here was mediated by endogenous CaCC activity.

The activation of CaCC might indicate that the calcium dynamics are somewhat altered in PLCζ-expressing *Xenopus* oocytes. We then monitored calcium dynamics by expressing G-CaMP 8 [23], which is a genetically encoded calcium indicator (GECI), in combination with voltage-clamp recording (Fig. 1G). We found that the intracellular calcium level is highly dependent on the membrane potential change only in PLCζ-expressing *Xenopus* oocytes. By applying 10 s step pulses ranging from −30 to −120 mV with a holding potential of 0 mV, we observed that the intracellular calcium increases around -30 mV, and more hyperpolarization brings more calcium inside the cell in PLCζ-injected oocytes but not in uninjected control (Fig. 1G). We also found that this calcium influx was inhibited by a SOC inhibitor, 10 μM YM-58483 (Fig. S2), while IP_3 receptor inhibitor, 3 μM Xestospongin C did not affect the response (Fig. S3). These results suggest that SOC mediates the hyperpolarization-driven calcium responses in PLCζ-injected oocytes.

Consistent with the hyperpolarization-driven calcium responses, we confirmed that more hyperpolarized prepulses exhibited a more obvious outward current of CaCC at +50 mV test pulses in PLCζ-injected oocytes, which was blocked by Ani9 or extracellular calcium-free conditions (Fig. 1H). Taken together, we revealed that PLCζ injection in *Xenopus* oocytes induced voltage-dependent calcium influx via SOC; hyperpolarization brings more calcium into the cells (Fig. 1I).

3.2. PLCζ induces voltage- and calcium-dependent PLC activity in Xenopus oocytes

Because PLCζ induces hyperpolarization-mediated calcium influx in *Xenopus* oocytes, and PLCζ is highly sensitive to the intracellular calcium level, we speculated that PLCζ activity might also be voltage-dependent in the PLCζ-expressing oocytes. To examine this possibility, we monitored the plasma membrane PIP_2 level using PHPLCδ-GFP, a well-known PIP_2 probe [24], in combination with TEVC (Fig. 2A). When we applied a step pulse from 0 to −90 mV in PLCζ-expressing oocytes in ND100 with 3 mM extracellular calcium, it significantly reduced the GFP signal compared with the non-PLCζ-injected control, indicating that PLCζ activity is upregulated by hyperpolarization (Fig. 2A and B). We also

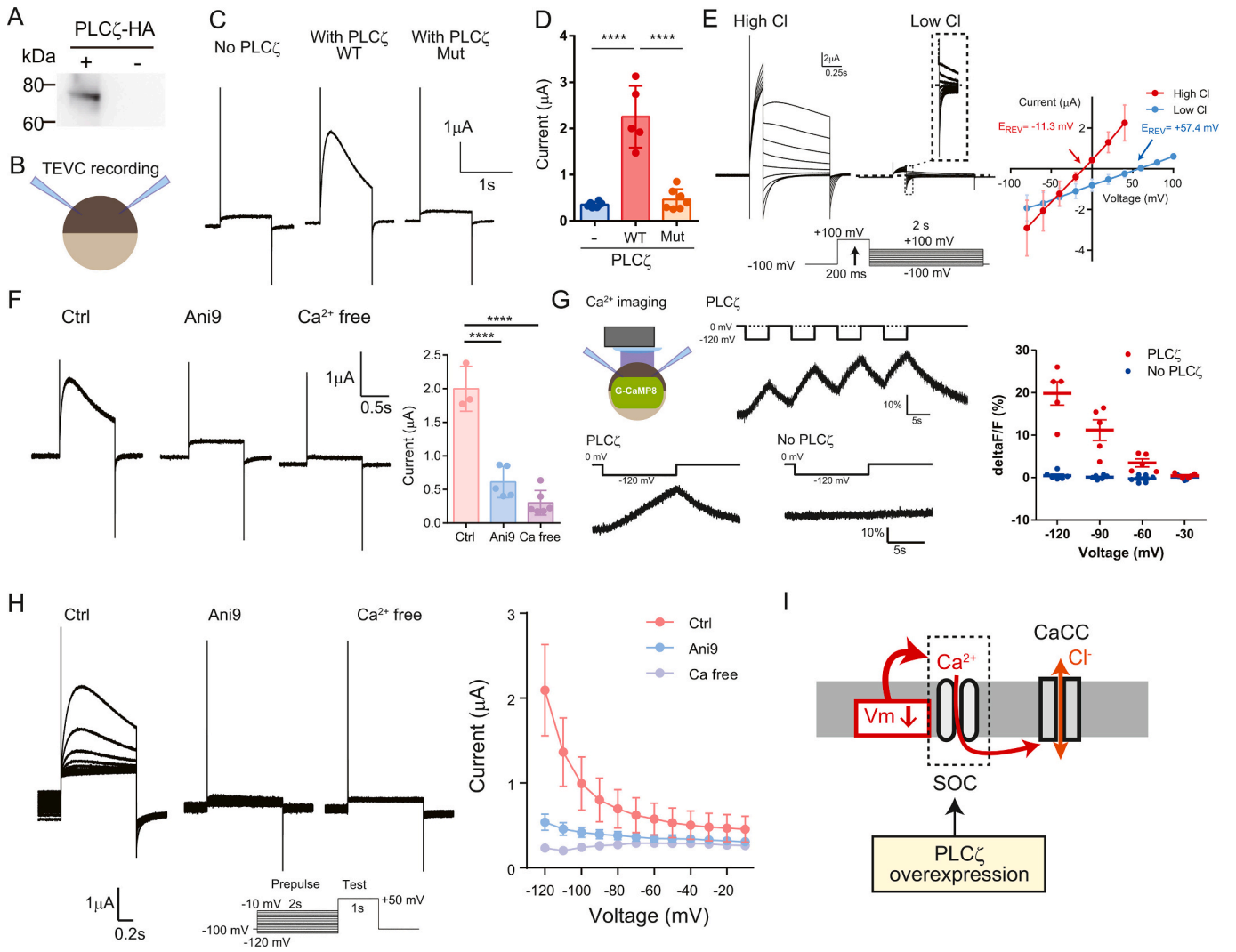

Fig. 1. Phospholipase C (PLC)ζ regulates the intracellular calcium levels and controls calcium-activated Cl^- channel (CaCC) activity in *Xenopus* oocytes. (A) Immunoblotting results for PLCζ-HA. This signal was specifically observed in PLCζ-HA-injected oocytes. (−), uninjected oocytes. (B) Two-electrode voltage-clamp recordings were conducted using ND96. (C) Representative traces of voltage-dependent currents in the uninjected, PLCζ-WT or PLCζ-mutant injected oocytes. The holding potential was maintained at −100 mV, and a depolarizing pulse of +50 mV was applied for 1 s. (D) Statistical analysis of current amplitudes induced in (C). Tukey's test was used for analysis. ****$p < 0.0001$. $N = 6$, 5 and 7 for uninjected, PLCζ-WT or PLCζ-mutant injected oocytes, respectively. (E) Reversal potential estimation protocol: The membrane potential was stepped from −100 to +100 mV for 200 ms to activate CaCC. Subsequently, it was changed to different values ranging from −100 to +100 mV for 2 s; dotted area shows the magnified trace. Right panel illustrates the current–voltage relationship in high and low Cl^- conditions. (F) Impact of Ani9 or Ca^{2+}-free bath solution on CaCC current in PLCζ-expressing cells. The holding potential was −100 mV, and a depolarizing pulse of +50 mV was applied for 1 s. Right panel shows the statistical analysis of the current amplitudes. Dunnet's test was used for analysis. $N = 3$, 5, and 6 for the control-, Ani9-, and Ca^{2+}-free cells, respectively. ****$p < 0.0001$. (G) Calcium imaging experiments using G-CaMP 8. The voltage protocol and representative fluorescence signals are shown. Fluorescence signal changes were consistent with the voltage changes only in PLCζ-expressing cells. The right panel depicts the plots of delta F/F (%) in PLCζ- and non-PLCζ-expressing cells. Red and blue dots indicate PLCζ ($n = 5$) and no PLCζ ($n = 6$), respectively. (H) CaCC recording with different voltage prepulses: A 2-s prepulse ranging from −120 mV to +10 mV was applied, followed by the test pulse (+50 mV for 1 s). Effects of Ani9 and Ca^{2+}-free bath solutions were determined. Representative traces and voltage protocols are shown on the left. Right-hand panel shows the average values obtained at different voltages. $N = 7$, 6, and 4 for the control, Ani9, and Ca^{2+}-free cells, respectively. (I) Schematic of CaCC activation. (For interpretation of the references to colour in this figure legend, the reader is referred to the web version of this article.)

observed the clear voltage-response curve in PLCζ-expressing oocytes; it started to show the reduction of PIP_2 at −30 mV and was maximized at −90 mV. This range is consistent with the range in which calcium influx occurs because of potential changes, as shown in Fig. 1G, suggesting that calcium influx from outside the cell may enhance PLCζ activity.

To test this possibility, we also examined the extracellular calcium dependency of PLCζ activity in *Xenopus* oocytes. As expected, Ca^{2+}-free conditions abolished the hyperpolarization-induced fluorescence change caused by PLCζ activity (Fig. 2E and F; a step pulse was applied from 0 to −60 mV). In contrast, increasing the extracellular calcium from 1 mM to 10 mM gradually enhanced PLCζ activity (Fig. 2E and F). These results indicate that the strength of PLCζ activity can be controlled by regulating extracellular calcium concentrations.

3.3. PLCζ regulates the PIP_2-sensitive KCNQ2/3 channel activity in a voltage- and calcium-dependent manner

Because we observed that PLCζ could regulate PIP_2 level in a voltage- and calcium-dependent manner, we wondered if this methodology is applicable to examining the regulatory mechanism of ion channel activity by PIP_2. KCNQ2/3 is the most representative K^+ channel, whose activity is positively regulated by PIP_2 [5,6]. Therefore, KCNQ2/3 was

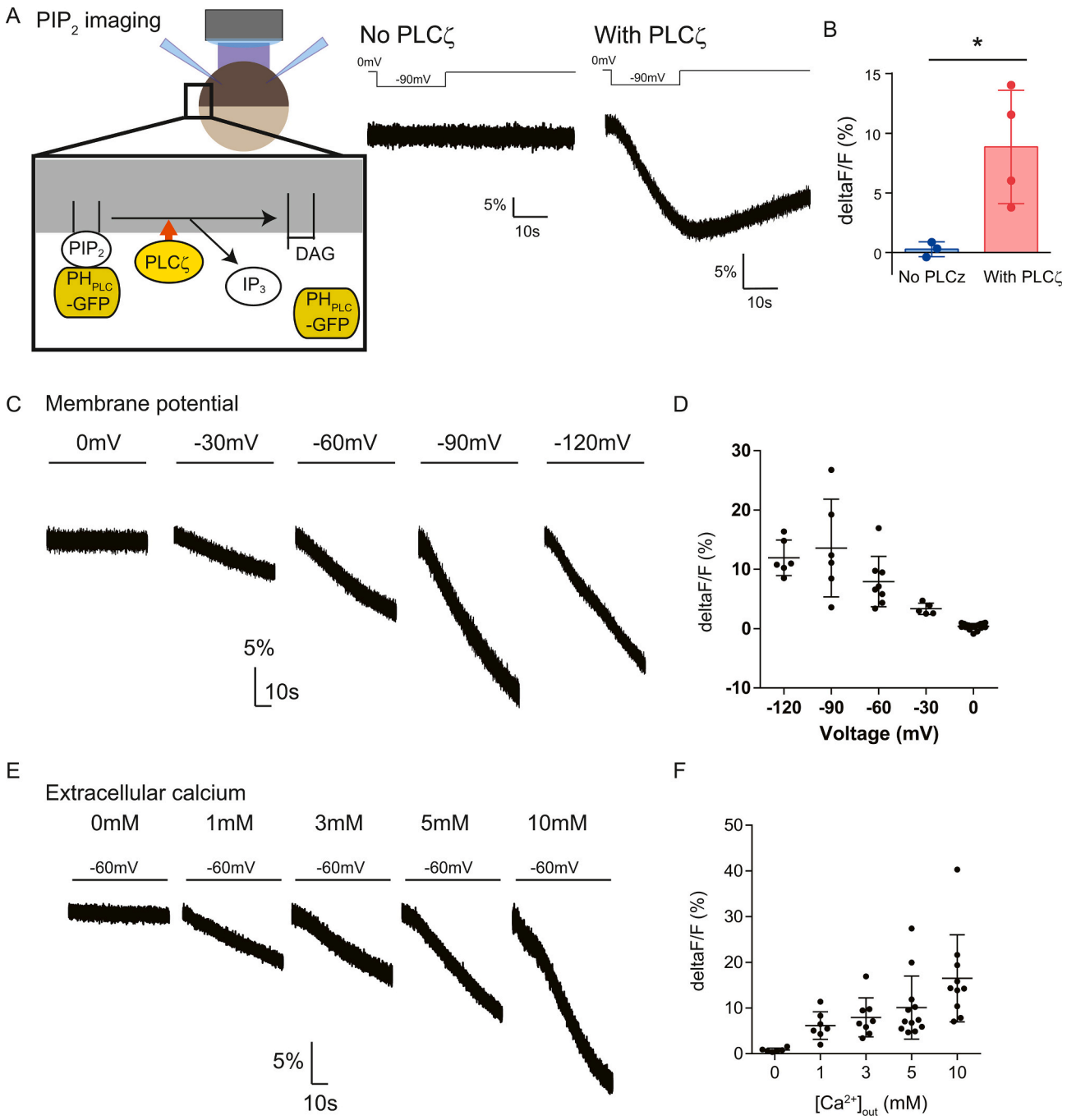

Fig. 2. PLCζ modulates the plasma membrane phosphatidylinositol 4,5-bisphosphate (PIP_2) levels in a voltage- and calcium-dependent manner. (A) Plasma membrane PIP_2 levels were monitored using PHPLCδ-GFP, a well-established PIP_2 probe. The membrane potential was stepped from 0 to −90 mV for 20 s to activate PLCζ. Representative traces are shown. (B) Statistical analysis of the deltaF/F(%) change in non-PLCζ- and PLCζ-expressing cells. Unpaired *t*-test was used for analysis. $*p < 0.05$. $N = 3$ and 4 for non-PLCζ- and PLCζ-expressing oocytes, respectively. (C) Impact of membrane potential changes on PIP_2 levels in PLCζ-expressing cells. The holding potential was set at 0 mV, and a 60-s hyperpolarization ranging from 0 to −120 mV was applied. Here, 3 mM Ca^{2+} ND100 was used. $N = 6, 6, 8, 5$, and 18 for −120, −90, −60, −30, and 0 mV, respectively. (D) Graph illustrating the relationship between deltaF/F(%) and membrane potential changes. (E) Influence of extracellular calcium on PIP_2 levels in PLCζ-expressing cells. The membrane potential was changed from 0 to −60 mV for 60 s, and the extracellular calcium concentration was changed from 0 to 10 mM. ND100 with the indicated Ca^{2+} solution was used. (F) Graph showing the relationship between deltaF/F(%) and extracellular calcium concentration. N = 6, 7, 8, 12, and 10 for 0, 1, 3, 5, and 10 mM $[Ca^{2+}]_{out}$, respectively.

expressed in independent experimental groups with or without PLCζ to determine whether PLCζ can regulate KCNQ2/3 activity. We held the membrane potential at −60 mV for >1 min to activate PLCζ and applied a 45-s + 50 mV depolarizing pulse to activate KCNQ2/3 as well as to inactivate PLCζ in *Xenopus* oocytes. As previously reported [25], KCNQ2/3 alone showed a slow outward current with voltage-dependent activation and almost no inactivation (Fig. 3A). On the other hand, when we co-expressed KCNQ2/3 with PLCζ, there was a slow rise of the outward current during the depolarization that was not observed without PLCζ (Fig. 3A). The current amplitude was approximately two-fold at the end of the recording compared to that at the beginning. This result suggests that PLCζ activity is much reduced during the depolarization in consistent with the idea that calcium influx is inhibited at this voltage. Thus, depolarization recovers the reduced plasma membrane PIP_2

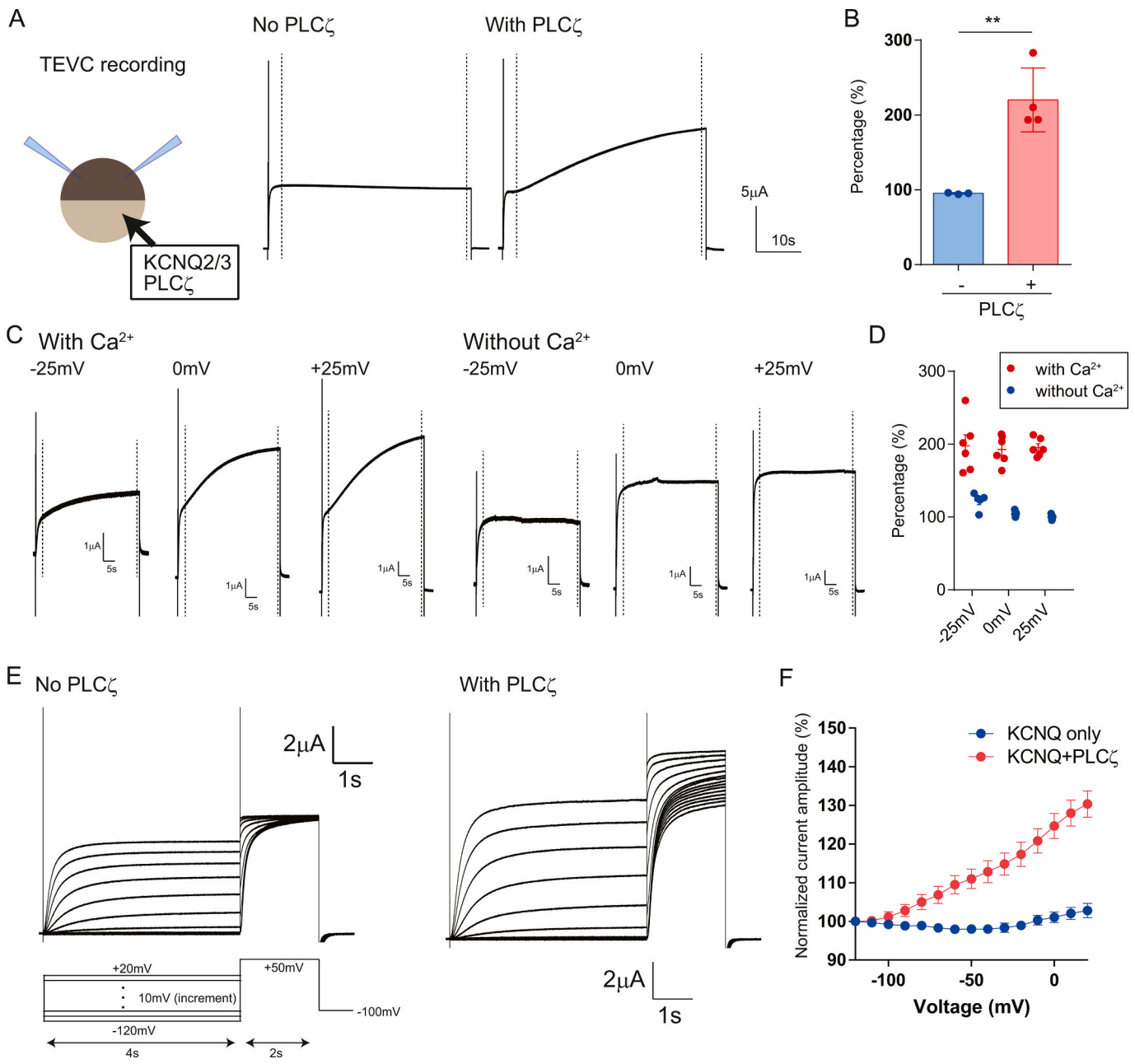

Fig. 3. PLCζ modulates KCNQ2/3 activity in a voltage- and calcium-dependent manner. (A) Two-electrode voltage clamp recordings were performed, maintaining the membrane potential at −60 mV, and + 50 mV depolarization was applied for 45 s. Dotted lines indicate the time points when the current amplitude was measured at the beginning (3 s) and end (44 s) of depolarization, respectively. (B) Statistical analysis of the percentage change in KCNQ2/3 current in non-PLCζ- and PLCζ-expressing cells. Current amplitude at the end (44 s) of depolarization was normalized to that at the beginning (3 s). Unpaired *t*-test was used for analysis. $^{**}p < 0.01$. N = 3 and 4 for non-PLCζ- and PLCζ-expressing cells, respectively. (C) Effect of extracellular calcium on KCNQ2/3 currents at different voltages. The protocol is the same as that shown in (A). (D) Graph illustrating the relationship between the percentage change in current and membrane potential. Red and blue dots indicate conditions with ($n = 6$) and without ($n = 5$) calcium, respectively. (E) Effect of a 4-s prepulse on KCNQ2/3 current amplitude. The pulse protocol is shown at the bottom, and current amplitude at +50 mV test pulse was measured. (F) Relationship between current amplitude and membrane potential of the prepulse. Data were obtained from (E). Current amplitude was normalized to that at −120 mV. N = 6 for both groups. (For interpretation of the references to colour in this figure legend, the reader is referred to the web version of this article.)

concentration and restores KCNQ2/3 activity.

When we applied the depolarizing pulse ranging from −25 mV to +25 mV with 25 mV increments, again we observed the slow large increase of KCNQ2/3 current with PLCζ co-expression. However, we did not observe this increase at any voltage examined under Ca^{2+}-free conditions (82 mM NaCl, 2 mM KCl, 5 mM HEPES, 5 mM $MgCl_2$ and 0.1 mM EGTA; Fig. 3C and D), indicating that extracellular Ca^{2+} is necessary for this process.

Next, to further investigate the relationship between the voltage and PLCζ activity, we applied a 4 s-prepulse to change PLCζ activity followed by the +50 mV test pulse (Fig. 3E and F). Without PLCζ, the amplitude of KCNQ2/3 was almost similar at any voltage of prepulse. On the other hand, the application of prepulse significantly affected the amplitude of KCNQ2/3 with PLCζ as shown in Fig. 3E. The difference begins to be visible at about -80 mV, and the difference gradually increases with more depolarization (Fig. 3F).

Overall, our data indicate that the activity of PIP_2-sensitive KCNQ2/3 is reliably regulated by PLCζ in a voltage- and calcium-dependent

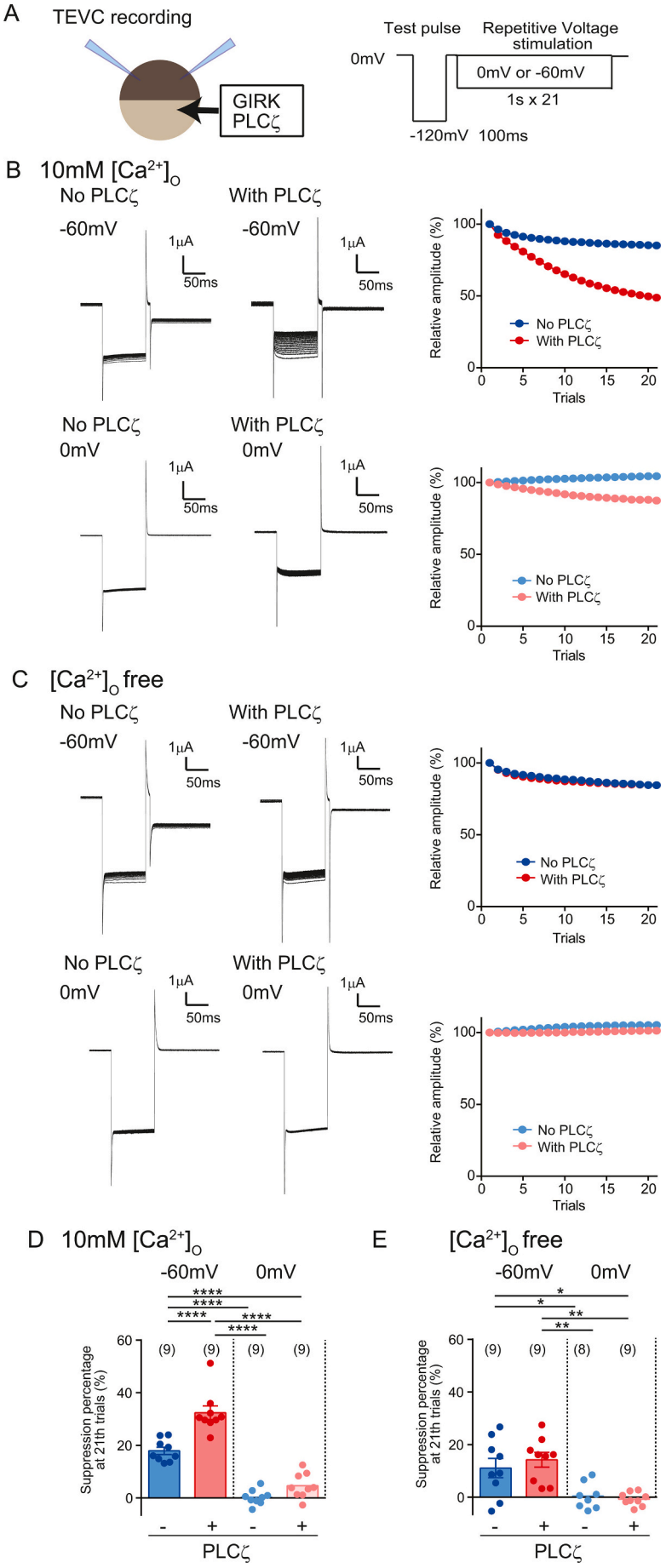

(caption on next page)

Fig. 4. PLCζ modulates GIRK activity in a voltage- and calcium-dependent manner. (A) Two-electrode voltage clamp recordings were performed to measure the GIRK channel activity. The voltage protocol is shown in the right panel. GIRK was activated at the test pulse (−120 mV for 100 ms). A repetitive 1-s depolarizing pulse was applied 21-times. The interval between each trace was set to 1.2 s. (B—C) GIRK experiments under 10 mM extracellular calcium (B) and extracellular calcium-free (C) conditions. Representative traces (*Left*) and time course (*right*) of GIRK current amplitude over 21 trials are shown. –60 mV (*top*) or 0 mV (*bottom*); repetitive stimulation was performed for non-PLCζ- or PLCζ-expressing oocytes. On the right, current amplitude was normalized to the value observed in the 1 st trial. (D–E) Statistical analysis of suppression percentage of GIRK current at the 21st trial. The results under 10 mM extracellular calcium (D) or extracellular calcium-free (E) conditions are shown. Tukey's test was used for analysis. *$p < 0.05$, **$p < 0.01$, and ****$p < 0.0001$. N is shown in parentheses.

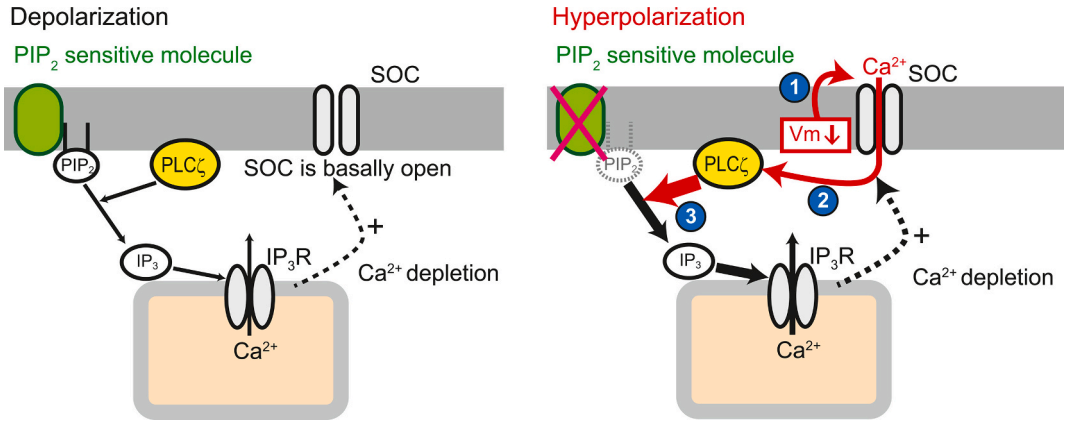

Fig. 5. Schematic illustration of voltage-dependent PLCζ activity in *Xenopus* oocytes. *Left*, introduction of PLCζ in *Xenopus* oocytes opened the store-operated calcium (SOC) channels at the depolarized state, as depletion of Ca^{2+} stores activates SOC (dotted arrow). However, calcium influx through the SOC was low because of the limited driving force of calcium. (1) Hyperpolarization augmented the driving force for calcium influx through SOC, (2) further enhancing calcium-sensitive PLCζ activity. (3) Enhanced PLCζ activity reduced the plasma membrane PIP_2 levels, modulating the PIP_2-sensitive membrane proteins.

manner, highlighting the potential of this molecule as a novel tool for PIP_2 manipulation.

3.4. PLCζ regulates the PIP_2-sensitive GIRK channel activity in a voltage- and calcium-dependent manner

We also investigated the potential effectiveness of PLCζ on ion channels other than KCNQ2/3, such as GIRK, which is another well-characterized ion channel known for its dependence on PIP_2 [26,27]. The holding potential was set at 0 mV to suppress PLCζ activity, and we monitored GIRK current using a −120 mV 100 ms test pulse. A low concentration of Cl^- ND96 was used to minimize the CaCC current. A 1 s voltage stimulus of 0 or 60 mV was repeatedly applied to keep or promote PLCζ activity with a sweep interval of 1.2 s (Fig. 4A).

In both 10 and 0 mM extracellular calcium conditions, GIRK current was slightly reduced by −60 mV repetitive stimulation even without PLCζ co-expression (Fig. 4B *top-left*, C *top-left*, and D), possibly due to some endogenous properties of the GIRK channel. In contrast, in the 10 mM $[Ca^{2+}]_{out}$ condition, repetitive stimulation of −60 mV caused a greater reduction in GIRK current in the PLCζ-expressing group than in the non-PLCζ-expressing group (Fig. 4B *top*). This PLCζ effect on GIRK current at −60 mV is not as great under the 0 mV repetitive pulse condition (Fig. 4B *bottom* and D). These results suggest that PLCζ activity induced by hyperpolarization is responsible for the reduction of GIRK current in 10 mM extracellular calcium condition. When the same experiment was performed under extracellular calcium-free conditions, no significant differences were observed between the PLCζ-expressing and non-PLCζ-expressing groups under both −60 and 0 mV conditions (Fig. 4C and E), further confirming that PLCζ activity is dependent on extracellular calcium levels.

4. Discussion

In the present study, we unexpectedly found that PLCζ-injected oocytes exhibited hyperpolarization-induced calcium influx, activating PLC activity. This calcium influx is dependent on extracellular calcium and appears to be mediated by SOC channels positively regulated by PLCζ expression. PLC activity in *Xenopus* oocytes can be easily regulated in a voltage- and calcium-dependent manner, making it applicable to the regulation of ion channel activity. Thus, we propose a novel methodology for examining ion channel PIP_2 sensitivity in *Xenopus* oocytes.

4.1. Mechanism underlying voltage-dependent PLCζ activation in *Xenopus* oocytes

Here, we found that voltage-dependent PLC activity could be induced just by injecting PLCζ cRNA into *Xenopus* oocytes. We found that hyperpolarization-driven calcium entry and accompanying CaCC activity could be induced in PLCζ-injected oocytes. This response was very similar to previous findings in IP_3-injected oocytes [21,28]. By directly injecting IP_3, a calcium response was observed via hyperpolarization, similar to the range of membrane potentials used in the present study. Similarly, they observed high CaCC activity, which was not observed without IP_3 [21,28]. They also confirmed that SOC mediated Ca^{2+} influx driven by hyperpolarization. Because PLC activity could cleave PIP_2 to produce IP_3, we suppose that the basal level of PLCζ activity somewhat reduces ER luminal Ca^{2+} concentrations, activating SOC in the plasma membrane (Fig. 5, *left*). Indeed, in the present study, the hyperpolarization-driven Ca^{2+} influx was inhibited by a SOC inhibitor (Fig. S2). Because Ca^{2+} influx promotes PLCζ activity, this machinery confers voltage- and extracellular Ca^{2+}-dependent PLC activity to *Xenopus* oocytes (Fig. 5, *right*), which is applicable to ion channel research.

4.2. PLCζ is a novel molecular tool to examine the PIP_2-sensitivity of ion channels

Here, we discovered that PLCζ is available to examine the PIP_2-sensitivity of ion channels. Several methodologies have been developed to accomplish the PIP_2 regulation [8,10,11]. For example, inside-out patch-clamp recording with the application of PIP_2 to the inner leaflet is the most quantitative method and can provide information on the PIP_2

dose-dependency curve [29]. However, because people use exogenous, in most cases, soluble PIP_2, in this experiment, the mechanism of its action on ion channels may be different from that of endogenous PIP_2. Some results obtained using this method are inconsistent with the results of other techniques targeting endogenous PIP_2 [30]. On the other hand, all other methodologies (VSP, G_qPCR, PJ, CRY2/CIBN, and PLCζ) target endogenous PIP_2 levels. Individual methods are designed based on different mechanisms and principles and hence have advantages and disadvantages. A summary of the characteristics of each technique is presented in Table 1.

One of the advantages of PLCζ among these techniques is that we do not need any other instrument than the TEVC system for manipulating PIP_2, and we can analyze ion channel activity alongside controllable PLC pathway. Among the above-mentioned tools, only VSP, aside from PLCζ, possesses this advantage. One advantage of PLCζ over VSP is that it could cleave PIP_2 to make IP_3 and there is no upregulation of PIP. Several reports have suggested that some ion channels may be sensitive to different types of Phosphoinositides (PIPs) [31,32]. Therefore, if the ion channel is sensitive to PIP and PIP_2, it becomes more difficult to detect the current change caused by VSP activation, which converts PIP_2 to PIP. Furthermore, we encountered difficulties performing G_qPCR on *Xenopus* oocytes. Because PLCζ has a common pathway with G_qPCR signaling, PLCζ could be an alternative technique that can easily mimic the G_qPCR pathway.

4.3. Tips for the application of PLCζ methodology to analyze the PIP_2-sensitivity of diverse ion channels

Here, we would like to outline the advantages and disadvantages of using PLCζ to analyze the PIP_2-sensitivity of ion channels. First, PLCζ needs intracellular calcium for activation. Therefore, this method cannot be used for calcium-activated ion (e.g., BK and TMEM16A) and voltage-gated calcium channels, which bring calcium into the cells at a depolarized membrane potential.

CaCC levels are highly upregulated in PLCζ-injected oocytes. Although the expression of CaCC indicates that PLCζ is successfully expressed in the oocytes, it can also mask the measurement of the targeting current depending on the voltage protocol. Here, we would like to offer some tips based on our measurements using PLCζ. As shown in Fig. 1E, CaCCs were hardly observed even in ND96 at potentials higher than −60 mV. Therefore, it is unnecessary to consider CaCC when the observation of the target channel falls within this potential range. If a membrane potential of less than −60 mV is needed, as is the case for GIRK recording, CaCC amplitude should be minimized by excluding Cl^- from the extracellular solution. Ani9, which efficiently inhibits TMEM16A activity, can be used to examine Cl^--permeable channel activity without removing Cl^- from the solution.

5. Conclusion

In conclusion, this study demonstrated that simple expression of PLCζ in *Xenopus* oocytes facilitates the easy exploration of the PIP_2 sensitivity of ion channels. Moreover, our technique expands the currently available analytical approaches for ion channel–lipid correlation analysis, contributing to further research in this field.

Declaration of generative AI and AI-assisted technologies in the writing process

During the preparation of this study, the authors used ChatGPT (OpenAI) in order to improve grammar and language clarity. After using this tool, the authors reviewed and edited the content as needed and take full responsibility for the content of the publication.

Funding

Funding was provided by Grants-in-Aid from JSPS (20K07274, 20KK0376) and the JST FOREST Program, Grant Number JPMJFR225Z (to T.K.). Financial support was received from The Ichiro Kanehara Foundation, Hyogo Science and Technology Association, the Sumitomo Foundation, the Ono Medical Research Foundation, the Uehara Memorial Foundation, Senri Life Science Foundation, Takeda Science Foundation, and Mochida Memorial Foundation for Medical and Pharmaceutical Research, all of which contributed to this research (to T.K.). We also acknowledge the support from JSPS (22H02804 to Y.O.), Core Research for Evolutional Science and Technology, Japan Science and Technology Agency (CREST, JST) (JPMJCR14M3 to Y.O.), and the Mitsubishi Foundation (to Y.O.).

CRediT authorship contribution statement

Takafumi Kawai: Writing – review & editing, Writing – original draft, Visualization, Supervision, Methodology, Investigation, Funding acquisition, Formal analysis, Data curation, Conceptualization. **Natsuki Mizutani:** Writing – review & editing, Investigation, Formal analysis, Data curation. **Yasushi Okamura:** Writing – review & editing, Supervision.

Declaration of competing interest

The authors declare no conflicts of interest.

Acknowledgments

We express our gratitude to Ms. Hikari Ginama and Ms. Megumi Kobayashi (Osaka university) for technical support.

Appendix A. Supplementary data

Supplementary data to this article can be found online at https://doi.org/10.1016/j.bbamem.2024.184396.

Data availability

All data relevant to this study are included within this article.

References

[1] T. Balla, Phosphoinositides: tiny lipids with giant impact on cell regulation, Physiol. Rev. 93 (2013) 1019–1137.
[2] G. Di Paolo, P. De Camilli, Phosphoinositides in cell regulation and membrane dynamics, Nature 443 (2006) 651–657.
[3] B.C. Suh, B. Hille, PIP_2 is a necessary cofactor for ion channel function: how and why? Annu. Rev. Biophys. 37 (2008) 175–195.
[4] B. Hille, E.J. Dickson, M. Kruse, O. Vivas, B.C. Suh, Phosphoinositides regulate ion channels, Biochim. Biophys. Acta 1851 (2015) 844–856.
[5] D.A. Brown, P.R. Adams, Muscarinic suppression of a novel voltage-sensitive K+ current in a vertebrate neurone, Nature 283 (1980) 673–676.
[6] B.C. Suh, B. Hille, Recovery from muscarinic modulation of M current channels requires phosphatidylinositol 4,5-bisphosphate synthesis, Neuron 35 (2002) 507–520.
[7] T. Kawai, Y. Okamura, Spotlight on the binding affinity of ion channels for Phosphoinositides: from the study of sperm flagellum, Front. Physiol. 13 (2022) 834180.
[8] Y. Okamura, A. Kawanabe, T. Kawai, Voltage-sensing phosphatases: biophysics, physiology, and molecular engineering, Physiol. Rev. 98 (2018) 2097–2131.
[9] T. Kawai, H. Miyata, H. Nakanishi, S. Sakata, S. Morioka, J. Sasaki, M. Watanabe, K. Sakimura, T. Fujimoto, T. Sasaki, M. Ikawa, Y. Okamura, Polarized PtdIns(4,5)P (2) distribution mediated by a voltage-sensing phosphatase (VSP) regulates sperm motility, Proc. Natl. Acad. Sci. U. S. A. 116 (2019) 26020–26028.
[10] Y. Yudin, L. Liu, J. Nagwekar, T. Rohacs, Methods to study phosphoinositide regulation of ion channels, Methods Enzymol. 652 (2021) 49–79.
[11] O. Idevall-Hagren, P. De Camilli, Detection and manipulation of phosphoinositides, Biochimica et Biophysica Acta - Molecular and Cell Biology of Lipids 2015 (1851) 736–745.

[12] Y. Murata, H. Iwasaki, M. Sasaki, K. Inaba, Y. Okamura, Phosphoinositide phosphatase activity coupled to an intrinsic voltage sensor, Nature 435 (2005) 1239–1243.
[13] G.R. Hammond, M.J. Fischer, K.E. Anderson, J. Holdich, A. Koteci, T. Balla, R. F. Irvine, PI4P and PI(4,5)P_2 are essential but independent lipid determinants of membrane identity, Science 337 (2012) 727–730.
[14] B.C. Suh, T. Inoue, T. Meyer, B. Hille, Rapid chemically induced changes of PtdIns (4,5)P2 gate KCNQ ion channels, Science 314 (2006) 1454–1457.
[15] O. Idevall-Hagren, E.J. Dickson, B. Hille, D.K. Toomre, P. De Camilli, Optogenetic control of phosphoinositide metabolism, Proc. Natl. Acad. Sci. U. S. A. 109 (2012) E2316–E2323.
[16] Z. Kouchi, K. Fukami, T. Shikano, S. Oda, Y. Nakamura, T. Takenawa, S. Miyazaki, Recombinant phospholipase Czeta has high Ca2+ sensitivity and induces Ca2+ oscillations in mouse eggs, J. Biol. Chem. 279 (2004) 10408–10412.
[17] C.M. Saunders, M.G. Larman, J. Parrington, L.J. Cox, J. Royse, L.M. Blayney, K. Swann, F.A. Lai, PLC zeta: a sperm-specific trigger of ca(2+) oscillations in eggs and embryo development, Development 129 (2002) 3533–3544.
[18] M. Prakriya, R.S. Lewis, Store-operated calcium channels, Physiol. Rev. 95 (2015) 1383–1436.
[19] M. Nomikos, A. Mulgrew-Nesbitt, P. Pallavi, G. Mihalyne, I. Zaitseva, K. Swann, F. A. Lai, D. Murray, S. McLaughlin, Binding of phosphoinositide-specific phospholipase C-zeta (PLC-zeta) to phospholipid membranes: potential role of an unstructured cluster of basic residues, J. Biol. Chem. 282 (2007) 16644–16653.
[20] Y. Murata, Y. Okamura, Depolarization activates the phosphoinositide phosphatase Ci-VSP, as detected in Xenopus oocytes coexpressing sensors of PIP_2, J. Physiol. 583 (2007) 875–889.
[21] K. Machaca, H.C. Hartzell, Reversible Ca gradients between the subplasmalemma and cytosol differentially activate Ca-dependent Cl currents, J. Gen. Physiol. 113 (1999) 249–266.
[22] K.L. Wozniak, W.A. Phelps, M. Tembo, M.T. Lee, A.E. Carlson, The TMEM16A channel mediates the fast polyspermy block in Xenopus laevis, J. Gen. Physiol. 150 (2018) 1249–1259.
[23] M. Ohkura, T. Sasaki, J. Sadakari, K. Gengyo-Ando, Y. Kagawa-Nagamura, C. Kobayashi, Y. Ikegaya, J. Nakai, Genetically encoded green fluorescent Ca2+ indicators with improved detectability for neuronal Ca2+ signals, PloS One 7 (2012) e51286.
[24] T.P. Stauffer, S. Ahn, T. Meyer, Receptor-induced transient reduction in plasma membrane PtdIns(4,5)P2 concentration monitored in living cells, Current Biology 8 (1998) 343–346.
[25] H.S. Wang, Z. Pan, W. Shi, B.S. Brown, R.S. Wymore, I.S. Cohen, J.E. Dixon, D. McKinnon, KCNQ2 and KCNQ3 potassium channel subunits: molecular correlates of the M-channel, Science 282 (1998) 1890–1893.
[26] C.L. Huang, S. Feng, D.W. Hilgemann, Direct activation of inward rectifier potassium channels by PIP_2 and its stabilization by Gbetagamma, Nature 391 (1998) 803–806.
[27] Y. Niu, X. Tao, K.K. Touhara, R. MacKinnon, Cryo-EM analysis of PIP(2) regulation in mammalian GIRK channels, eLife 9 (2020).
[28] R. Courjaret, K. Machaca, Xenopus oocyte as a model system to study store-operated Ca(2+) entry (SOCE), Front. Cell Dev. Biol. 4 (2016) 66.
[29] H. Zhang, L.C. Craciun, T. Mirshahi, T. Rohacs, C.M. Lopes, T. Jin, D.E. Logothetis, PIP_2 activates KCNQ channels, and its hydrolysis underlies receptor-mediated inhibition of M currents, Neuron 37 (2003) 963–975.
[30] M. Kruse, G.R.V. Hammond, B. Hille, Regulation of voltage-gated potassium channels by PI(4,5)P_2, J. Gen. Physiol. 140 (2012) 189–205.
[31] X. Zhang, X. Li, H. Xu, Phosphoinositide isoforms determine compartment-specific ion channel activity, Proc. Natl. Acad. Sci. U. S. A. 109 (2012) 11384–11389.
[32] V. Lukacs, B. Thyagarajan, P. Varnai, A. Balla, T. Balla, T. Rohacs, Dual regulation of TRPV1 by phosphoinositides, The Journal of Neuroscience 27 (2007) 7070–7080.